BMB Reports - Manuscript Submission

Manuscript Draft

Manuscript Number: BMB-18-083

Title: Inactivation of Sirtuin2 protects mice from acetaminophen-induced liver injury: possible involvement of ER stress and S6K1 activation

Article Type: Article

Keywords: Sirtuin2; Acetaminophen; ER stress; S6K1; Hepatotoxicity

Corresponding Author: Soo Han Bae

Authors: Soo Han Bae[2,*], Da Hyun Lee[1,2,#], Buhyun Lee[1,2,#], Jeong Su Park[2], Yu Seol Lee[1,2], Jin Hee Kim[6], Yejin Cho[2], Yoonjung Jo[3], Hyun-Seok Kim[3], Yong-ho Lee[4,5], Ki Taek Nam[1,2]

Institution: [1]Brain Korea 21 PLUS Project for Medical Science, Yonsei University,
[2]Severance Biomedical Science Institute, Yonsei Biomedical Research Institute, Yonsei University College of Medicine, 50 Yonsei-ro, Seodaemun-gu, Seoul 03722, Republic of Korea,
[3]Department of Bioinspired Science, Ewha Womans University, Seoul 120-750, Korea,
[4]Division of Endocrinology and Metabolism, Department of Internal Medicine, Yonsei University College of Medicine, 50-1, Yonsei-ro, Seodaemun-gu, Seoul 03722, Republic of Korea,
[5]Institute of Endocrine Research, Yonsei University College of Medicine, 50-1, Yonsei-ro, Seodaemun-gu, Seoul 03722, Republic of Korea,
[6]Brain Korea 21 PLUS Project for Medical Science, Yonsei University College of Medicine, 50-1 Yonsei-ro, Seodaemun-gu, Seoul, 03722, Republic of Korea,

Manuscript Type: Article

Inactivation of Sirtuin2 protects mice from acetaminophen-induced liver injury: possible involvement of ER stress and S6K1 activation

Da Hyun Lee[a,b#], Buhyun Lee[a,b#], Jeong Su Park[b], Yu Seol Lee[a,b], Jin Hee Kim[f], Yejin Cho[b], Yoonjung Jo[c], Hyun-Seok Kim[c], Yong-ho Lee[d,e]*, Ki Taek Nam[a,b]*, and Soo Han Bae[b]*

[a]Brain Korea 21 PLUS Project for Medical Science, Yonsei University;

[b]Severance Biomedical Science Institute, Yonsei Biomedical Research Institute, Yonsei University College of Medicine, 50 Yonsei-ro, Seodaemun-gu, Seoul 03722, Republic of Korea;

[c]Department of Bioinspired Science, Ewha Womans University, Seoul 120-750, Korea;

[d]Division of Endocrinology and Metabolism, Department of Internal Medicine, Yonsei University College of Medicine, 50-1, Yonsei-ro, Seodaemun-gu, Seoul 03722, Republic of Korea;

[e]Institute of Endocrine Research, Yonsei University College of Medicine, 50-1, Yonsei-ro, Seodaemun-gu, Seoul 03722, Republic of Korea;

[f]Brain Korea 21 PLUS Project for Medical Science, Yonsei University College of Medicine, 50-1 Yonsei-ro, Seodaemun-gu, Seoul, 03722, Republic of Korea

[#]These authors contributed equally to this work.

Running Title: Sirt2 inhibition reduces APAP-induced liver injury

Corresponding authors:

Soo Han Bae, Ph. D

Severance Biomedical Science Institute, Yonsei Biomedical Research Institute, Yonsei University College of Medicine, 50-1 Yonsei-ro, Seodaemun-gu, Seoul 03722, Republic of Korea. Tel.: +82-2 2228-0756; Fax: +82-2-2227-8129; E-mail address: soohanbae@yuhs.ac

Ki Taek Nam, D.V.M, Ph. D

Severance Biomedical Science Institute, Yonsei Biomedical Research Institute, Yonsei University College of Medicine, 50-1 Yonsei-ro, Seodaemun-gu, Seoul 03722, Republic of Korea. Tel.: +82-2 2228-0754; Fax: +82-2-2227-8129; E-mail address: KITAEK@yuhs.ac

Yong-ho Lee, M.D., Ph.D.

Division of Endocrinology and Metabolism, Department of Internal Medicine, Yonsei University College of Medicine, 50-1, Yonsei–ro, Seodaemun–gu, Seoul 03722, Republic of Korea. Tel.: +82-2-2228-1943; Fax: +82-2-393-6884; E-mail address: yholee@yuhs.ac

Abstract

Acetaminophen (APAP) overdose can cause hepatotoxicity by inducing mitochondrial damage and subsequent necrosis in hepatocytes. Sirtuin2 (Sirt2) is an NAD^+-dependent deacetylase that regulates several biological processes, including hepatic gluconeogenesis, as well as inflammatory pathways. We show that APAP decreases the expression of Sirt2. Moreover, the ablation of Sirtuin2 attenuates APAP-induced liver injuries, such as oxidative stress and mitochondrial damage in hepatocytes. We found that Sirt2 deficiency alleviates the APAP -mediated endoplasmic reticulum stress and phosphorylation of the p70 ribosomal S6 kinase 1 (S6K1). Moreover, Sirt2 interacts with and deacetylates S6K1, followed by S6K1 phosphorylation induction. This study elucidates the molecular mechanisms underlying the protective role of Sirt2 inactivation in APAP-induced liver injuries.

Keywords: Sirtuin2, Acetaminophen, ER stress, S6K1, Hepatotoxicity

Introduction

Drug-induced liver injury is a leading cause of acute liver failure. Therefore, the discovery of novel therapeutic targets for regulating the progression of liver injury is important (1). Acetaminophen (APAP) has been widely used to understand the mechanism of drug-induced hepatotoxicity as a major cause of liver damage.

APAP-mediated hepatotoxicity is caused by the cytochrome P450 (CYP) 1A2-, CYP2E1-, and CYP3A4-driven conversion of APAP into hepatotoxic metabolites (2-4). Moreover, APAP-induced hepatotoxicity is associated with oxidative stress induced by *N*-Acetyl-*p*-benzoquinone imine, a reactive metabolite of APAP (5) or by endoplasmic reticulum (ER) stress (6, 7).

Sirtuins are NAD^+-dependent deacetylases with seven isoforms (Sirt1-7) in mammals (8). Their functions are known to be associated with metabolic diseases, such as type II diabetes and obesity (9, 10). Among the seven isoforms, Sirtuin2 (Sirt2) may coordinate the regulation of several distinct metabolic processes, including adipocyte differentiation, fatty acid oxidation, hepatic gluconeogenesis, and insulin action, as well as the regulation of inflammatory pathways (11). Nevertheless, the role of Sirt2 in drug-induced liver injury remains unclear.

In this study, we investigated the role of Sirt2 in APAP-induced hepatotoxicity using mouse models in which Sirt2 was inactivated genetically and pharmacologically.

Results

APAP decreases Sirt2 levels and Sirt2 ablation ameliorates APAP-induced liver injuries in mice

APAP is usually deemed as a safe drug, but APAP intoxication after an overdose can cause massive hepatocellular necrosis and acute liver injury (2, 4, 5, 12). To investigate whether Sirt2 plays a role in APAP-induced liver injuries, we first determined Sirt2 levels in the mouse liver following treatment with APAP for the indicated periods of time. Our results showed that APAP treatment induced the degradation of Sirt2 isoforms 1 and 2 in the mouse liver (Fig. 1A, 1C-1D). However, the Sirt2 mRNA levels were not changed in the same samples (Fig. 1B). To verify whether Sirt2 degradation is regulated at the translational or post-transcriptional level, we treated normal liver cells (AML12 cells) with cycloheximide to inhibit protein synthesis and then measured Sirt2 levels in response to APAP-induced injuries. Sirt2 degradation was partially blocked in cycloheximide-treated AML12 cells (Supplementary Fig. 1A-1C), indicating that Sirt2 degradation is translationally modulated. We further examined whether downregulation of Sirt2 by APAP is mediated by the proteasomal or autophagic degradation pathway. AML12 cells were treated with an autophagy inhibitor (chloroquine, CQ) or a proteasome inhibitor (MG132). Immunoblot analysis showed that APAP-induced Sirt2 degradation was markedly inhibited by MG132 (Supplementary Fig. 1D-1F) and partially degraded by CQ (Supplementary Fig. 1G-1I). Taken together, these results indicate that APAP-induced downregulation of Sirt2 was regulated at the translational level and by the proteasomal degradation pathway. To investigate the effect of Sirt2 on APAP-induced liver injuries, we examined liver tissues from Sirt2 wild-type (WT) and Sirt2 knockout (KO) mice treated with APAP or vehicle for 12 h. Furthermore, B6 mice, pre-treated with AGK2, the most potent Sirt2 inhibitor (13-15), were

treated with APAP or vehicle to further examine whether the pharmacological inactivation of Sirt2 alleviates APAP-induced liver injuries. Subsequently, standard hematoxylin-eosin (H&E) staining and TUNEL analysis were performed. Histological analyses using H&E staining revealed that normal liver displayed prominent liver injuries and necrotic hepatic cell death. In contrast, histological sections from both Sirt2 KO mice (Fig. 1E) and mice treated with AGK2 (Fig. 1I) showed a decrease in the severity of liver injuries and necrotic hepatic cell death compared with Sirt2 WT mice in response to APAP. Moreover, TUNEL-positive apoptotic cells were scarcely detected in the livers of Sirt2 WT and Sirt2 KO mice treated with APAP or vehicle for 12 h. Our results showed a considerable decrease in the percentage of TUNEL-positive cells in the liver of Sirt2 KO mice (Fig. 1F) and mice treated with AGK2 (Fig. 1J) in response to APAP. Moreover, Sirt2 KO mice treated with APAP and mice treated with AGK2 exhibited decreased levels of alanine transaminase (GPT) and aspartate transaminase (GOP) in response to APAP (Fig. 1G and 1L). Correspondingly, Sirt2 KO mice treated with APAP for 6 h showed a substantial decrease in the size of necrotic areas, TUNEL-positive cell count, and GPT and GOP levels (Supplementary Fig. 2A-2F). Furthermore, we found that the level of protein 3-nitrotyrosine, a marker of oxidative stress, decreased in Sirt2 KO mice treated with APAP for 12 h (Supplementary Fig. 3A-3B) and 6 h (Supplementary Fig. 4A-4B), and in AGK2-treated livers (Supplementary Fig. 5A and 5B), compared to that in Sirt2 WT mice. Based on the notion that an APAP overdose significantly induces mitochondrial damage (16), we provide evidence that the ablation of Sirt2 and pharmacological inactivation of Sirt2 alleviate the APAP-induced mitochondrial damage, using electron microscopy. In the same samples, we found distinctive mitochondrial morphological changes, typical necrotic cells with swollen mitochondria, accumulation of lipid droplets, and disruption of plasma membranes (17) (Supplementary Fig. 3C and 5C).

Collectively, our data show that the pharmacological inactivation of Sirt2 in APAP-treated mouse livers exhibits effects similar to those of the pathology that results from the ablation of Sirt2.

The inactivation of Sirt2 attenuates ER stress in APAP-induced liver injuries in mice

It has been reported that APAP can induce ER stress *in vivo* and *in vitro* and that these deleterious effects can play a significant role in the APAP-induced cell death in the liver (6, 18-20). Upon acute ER stress, BiP/Grp78 dissociates from these sensors, leading to the activation of the unfolded protein response pathway, to resolve ER stress and restore homeostasis (21). Consistent with this report, we found that ER stress marker genes such as BiP/Grp78, PERK, ATF4, and IRE1α were also upregulated in the mouse liver (Fig. 2A-2D). To determine whether Sirt2 regulates the APAP-mediated increase in ER stress, we examined the levels of ER stress markers in Sirt2 WT and KO mice treated with APAP. APAP enhanced BiP/Grp78 levels and downregulated ER stress marker genes in Sirt2 KO mice (Fig. 2E-2H) and mice treated with AGK2 (Fig. 2I-2L), as assessed by qRT-PCR. Moreover, the short APAP treatment (6 h) showed a similar effect (Supplementary Fig. 6A-6E). Consistent with the notion that ablation of Sirt2 regulates the APAP-induced ER stress, these results suggest that inactivation of Sirt2 ameliorates the APAP-induced ER stress in the mouse liver.

The APAP-induced S6K1 phosphorylation is inhibited in the livers of Sirt2-inactivated mice

The mammalian target of rapamycin complex 1 (mTORC1) has been implicated in the regulation of ER stress, and the inhibition of mTORC1 may have potential therapeutic effects

in ER stress-related diseases (22). To investigate whether the ablation of Sirt2 ameliorates the APAP-induced ER stress through the regulation of the mTORC1 signaling pathway, the level of mTOR phosphorylation induced by APAP was determined by immunoblot analysis in Sirt2 WT and KO mice. Our results indicated that mTOR phosphorylation level did not differ between the two groups (Supplementary Fig. 7A-7D). S6K1 and ribosomal protein S6 are downstream targets of mTORC1. Chronic acetaminophen treatment increased S6K1 phosphorylation in rat muscles (23). To investigate whether Sirt2 regulates the S6K1 signaling pathway, we examined the levels of APAP-induced S6K1 phosphorylation in the livers of Sirt2 WT and KO mice and mice treated with AGK2. In accordance with the results obtained in rats, we observed that the phosphorylation of S6K1 and that of the S6 ribosomal protein gradually increased in a time-dependent manner following APAP treatment in the mouse liver (Fig. 3A-3C). Moreover, S6K1 phosphorylation was markedly decreased in Sirt2 KO mice treated with APAP for 12 h (Fig. 3D-3F), 6 h (Supplementary Fig. 6A-6B) and in mice treated with AGK2 (Fig. 3G-3I). These results confirmed that Sirt2 inactivation downregulates the APAP-induced ER stress by inhibiting the S6K1 signaling pathway.

Sirt2 regulates S6K1 phosphorylation through S6K1 deacetylation in APAP-treated mouse livers

It has been reported that S6K1 acetylation blocks the mTORC1-dependent S6K1 phosphorylation at T389, an essential phosphorylation site for S6K1 activity and that this acetylation is inhibited by Sirt2 (24). Therefore, we explored the mechanism underlying the Sirt2-mediated regulation of S6K1 acetylation in APAP-treated mouse livers. Firstly, to confirm the role of Sirt2 in S6K1 deacetylation, we performed a co-immunoprecipitation analysis on HEK293 cells transfected with expression vectors for S6K1 or HA-tagged S6K1,

together with a vector encoding a Flag-tagged Sirt2 (F-SIRT2). Consistent with the above report, our results showed that Sirt2 interacts with S6K1 (Fig. 4A and 4C). Furthermore, to validate that S6K1 deacetylation is mediated by Sirt2, we performed an acetylation assay coupled with co-immunoprecipitation in HEK293 cells transfected with expression vectors for the wild-type or a Sirt2 catalytic mutant (H187Y) and S6K1 or HA-tagged S6K1. Our results revealed that the Sirt2 catalytic mutant did not deacetylate S6K1, as opposed to the wild-type Sirt2 (Fig. 4B and 4D). In addition, we observed similar results using APAP-treated livers from Sirt2 knockout mice and AGK2-pretreated mice (Fig. 4E and 4F). Taken together, these results suggest that Sirt2 interacts with and deacetylates S6K1 to promotes its phosphorylation.

Discussion

In this study, we found that an APAP overdose decreased the expression of two Sirt2 proteins in the mouse liver. A sequence analysis, using the GenBank sequence database, showed that Sirt2 has four different human splice variants. However, only transcript variants 1 and 2 have been verified as protein isoforms of physiological relevance (25).

The observation that APAP may mediate the downregulation of Sirt2 proteins (isoforms 1 and 2) led us to investigate the role of Sirt2 in APAP-induced liver injuries. Our results revealed that the Sirt2 deficiency renders mice less susceptible to APAP-induced hepatotoxicity.

Recent screening campaigns have identified several selective inhibitors of Sirt2, including Sirt-rearranging ligands 1 and 2, AK-1, AK-7, and AGK2 (26, 27). Of these, AGK2 is the most potent inhibitor of Sirt2 (13, 15). Accordingly, we found that AGK2 treatment significantly alleviated the APAP-induced hepatotoxicity in the mouse liver.

Excessive ER stress results in multiple pathologies, including cirrhosis, non-alcoholic fatty liver disease, diabetes mellitus, viral inflammation, and cancer (28, 29). Previous studies have reported that APAP is able to induce ER stress *in vivo* and *in vitro* and that this deleterious effect could play a significant role in the APAP-induced cell death in the liver (6, 18-20). Our observation that the Sirt2 deficiency attenuates the APAP-induced ER stress might explain the protective role of Sirt2 inactivation in the APAP-induced hepatotoxicity.

It is widely known that mTORC1 regulates cellular processes, protein synthesis, cell growth, and survival through the phosphorylation and activation of S6K1 (30). Moreover, mTORC1 represents one of the upstream triggers of ER stress; hence. the inhibition of mTORC1 may potentially be employed in the therapy of ER stress-induced diseases (22). A previous study reported that mTOR/S6K signaling is inhibited by acetaminophen; however, this study was limited as primary mouse hepatocytes were used for the experiments (17, 31). On the contrary, there are several reports that S6K1 phosphorylation is increased by chronic APAP treatment in rats (23) and by APAP overdose in mouse livers (32, 33). Correspondingly, our results showed that the ablation of Sirt2 downregulates the APAP-induced S6K1 phosphorylation, resulting in an attenuation of ER stress. However, the inactivation of Sirt2 has no effect on the phosphorylation of mTORC1 (Supplementary Fig. 7). These observations suggest that S6K1 may be a specific substrate of Sirt2 in this context.

A recent study has shown that the acetylation of S6K1 blocks the mTORC1-dependent phosphorylation of S6K1 and that the acetylation of S6K1 is inhibited by Sirt2 (24). In agreement with this report, we also found that Sirt2 interacts with and deacetylates S6K1. Thus, Sirt2 inhibition induces S6K1 acetylation and subsequently block S6K1 phosphorylation to downregulate the APAP-induced ER stress in the mouse liver.

Growing evidence from recent studies indicates that the inactivation of Sirt2 has protective roles in liver diseases. For example, it has been reported that Sirt2 deficiency might attenuate the APAP-induced liver toxicity by downregulating c-Jun NH2-terminal kinase (JNK) activation. Furthermore, Sirt2 aggravates the hepatic ischemia-reperfusion injury through the deacetylation and inhibition of mitogen-activated protein kinase phosphatase-1 (34). Moreover, Sirt2 accelerates hepatic fibrogenesis by regulating the ERK/c-MYC pathway. Therefore, the inactivation of Sirt2 may represent an effective strategy for protecting against the development of hepatic fibrosis (35). In addition, the ablation of the Sirt3 mitochondrial deacetylase plays a protective role in APAP-induced hepatotoxicity through the activation of mitochondrial aldehyde dehydrogenase 2 (36).

Furthermore, Sirt2 knockdown induces autophagy and prevents post-slippage death by abnormally prolonging the mitotic arrest induced by microtubule inhibitors (37). Moreover, Sirt2 leads to genetic instability and tumorigenesis by positively regulating APC/C activity via the deacetylation of its coactivators, CDH1 and CDC20 (38, 39).

The silencing of Sirt2 significantly activates necrosis in PC12 cells but does not affect autophagy in these cells (40). Furthermore, the inhibition of Sirt2 induces p53-dependent apoptosis in cancer cells (41). In conclusion, Sirt2 plays different roles in various contexts, through the deacetylation of specific substrates.

Taken together, we have elucidated the molecular mechanism underlying the protective role of Sirt2 inactivation in APAP-induced liver injuries.

Materials and methods

See Supplementary Information for Materials and Methods.

Acknowledgments

We thank Dr. Chu-Xia Deng, Dr. S. G Rhee, and Dr. J. H. Ryu for providing the Sirt2 WT and Sirt2 KO mice. In addition, we thank S. H. Sung and S. Y. Oh for maintaining the Sirt2 WT and Sirt2 KO mice. This work was supported by the National Research Foundation of Korea (NRF-2017R1A2B4007400; S. H. Bae, NRF-2017R1D1A1B03032808; J. S. Park, NRF-2016R1A5A1010764; 2015R1C1A1A01052558; Y. H. Lee) and a Faculty Research Grant from the Yonsei University College of Medicine (6-2014-0068; S. H. Bae). It was also supported by a grant from the Korea Health Technology R&D Project through the Korea Health Industry Development Institute (KHIDI), funded by the Ministry of Health & Welfare, Republic of Korea (HI17C0913; HI16C0257; S. H. Bae, HI14C2476; Y. H. Lee). This research was also supported by the Korea Mouse Phenotyping Project (NRF-2016M3A9D5A01952416) from the National Research Foundation, by the Bio & Medical Technology Development Program of the NRF, funded by the Korean government (NRF-2017M3A9F3041234, NRF-2017R1A2B2009850) and the Brain Korea 21 PLUS Project for Medical Science, Yonsei University (to K. T. Nam).

Conflict of interest: The authors declare no conflict of interest.

References

1. Ghabril, M., Chalasani, N. and Bjornsson, E. (2010) Drug-induced liver injury: a clinical update. *Curr Opin Gastroenterol* **26,** 222-226.
2. James, L. P., Mayeux, P. R. and Hinson, J. A. (2003) Acetaminophen-induced

hepatotoxicity. *Drug metabolism and disposition: the biological fate of chemicals* **31,** 1499-1506.

3. Ni, H. M., Williams, J. A., et al. (2012) Targeting autophagy for the treatment of liver diseases. *Pharmacol Res* **66,** 463-474.
4. Hinson, J. A., Roberts, D. W. and James, L. P. (2010) Mechanisms of acetaminophen-induced liver necrosis. *Handbook of experimental pharmacology***,** 369-405.
5. Copple, I. M., Goldring, C. E., et al. (2008) The hepatotoxic metabolite of acetaminophen directly activates the Keap1-Nrf2 cell defense system. *Hepatology* **48,** 1292-1301.
6. Nagy, G., Kardon, T., et al. (2007) Acetaminophen induces ER dependent signaling in mouse liver. *Archives of biochemistry and biophysics* **459,** 273-279.
7. Foufelle, F. and Fromenty, B. (2016) Role of endoplasmic reticulum stress in drug-induced toxicity. *Pharmacology research & perspectives* **4,** e00211.
8. Frye, R. A. (2000) Phylogenetic classification of prokaryotic and eukaryotic Sir2-like proteins. *Biochem Biophys Res Commun* **273,** 793-798.
9. Morris, B. J. (2013) Seven sirtuins for seven deadly diseases of aging. *Free Radic Biol Med* **56,** 133-171.
10. Houtkooper, R. H., Pirinen, E. and Auwerx, J. (2012) Sirtuins as regulators of metabolism and healthspan. *Nature reviews. Molecular cell biology* **13,** 225-238.
11. Gomes, P., Outeiro, T. F. and Cavadas, C. (2015) Emerging Role of Sirtuin 2 in the Regulation of Mammalian Metabolism. *Trends Pharmacol Sci* **36,** 756-768.
12. Craig, D. G., Bates, C. M., et al. (2011) Overdose pattern and outcome in paracetamol-induced acute severe hepatotoxicity. *British journal of clinical pharmacology* **71,** 273-282.

13. Outeiro, T. F., Kontopoulos, E., et al. (2007) Sirtuin 2 inhibitors rescue alpha-synuclein-mediated toxicity in models of Parkinson's disease. *Science* **317,** 516-519.

14. Rumpf, T., Schiedel, M., et al. (2015) Selective Sirt2 inhibition by ligand-induced rearrangement of the active site. *Nature communications* **6,** 6263.

15. Luthi-Carter, R., Taylor, D. M., et al. (2010) SIRT2 inhibition achieves neuroprotection by decreasing sterol biosynthesis. *Proc Natl Acad Sci U S A* **107,** 7927-7932.

16. Hu, J., Ramshesh, V. K., et al. (2016) Low Dose Acetaminophen Induces Reversible Mitochondrial Dysfunction Associated with Transient c-Jun N-Terminal Kinase Activation in Mouse Liver. *Toxicological sciences : an official journal of the Society of Toxicology* **150,** 204-215.

17. Ni, H. M., Williams, J. A., Jaeschke, H. and Ding, W. X. (2013) Zonated induction of autophagy and mitochondrial spheroids limits acetaminophen-induced necrosis in the liver. *Redox Biol* **1,** 427-432.

18. Lorz, C., Justo, P., et al. (2004) Paracetamol-induced renal tubular injury: a role for ER stress. *Journal of the American Society of Nephrology : JASN* **15,** 380-389.

19. Uzi, D., Barda, L., et al. (2013) CHOP is a critical regulator of acetaminophen-induced hepatotoxicity. *Journal of hepatology* **59,** 495-503.

20. Kalinec, G. M., Thein, P., et al. (2014) Acetaminophen and NAPQI are toxic to auditory cells via oxidative and endoplasmic reticulum stress-dependent pathways. *Hearing research* **313,** 26-37.

21. Bertolotti, A., Zhang, Y., et al. (2000) Dynamic interaction of BiP and ER stress transducers in the unfolded-protein response. *Nat Cell Biol* **2,** 326-332.

22. Dong, G., Liu, Y., et al. (2015) mTOR contributes to ER stress and associated

apoptosis in renal tubular cells. *American journal of physiology. Renal physiology* **308,** F267-274.

23. Wu, M., Liu, H., et al. (2010) Acetaminophen improves protein translational signaling in aged skeletal muscle. *Rejuvenation research* **13,** 571-579.

24. Hong, S., Zhao, B., et al. (2014) Cross-talk between sirtuin and mammalian target of rapamycin complex 1 (mTORC1) signaling in the regulation of S6 kinase 1 (S6K1) phosphorylation. *J Biol Chem* **289,** 13132-13141.

25. Rack, J. G., VanLinden, M. R., et al. (2014) Constitutive nuclear localization of an alternatively spliced sirtuin-2 isoform. *J Mol Biol* **426,** 1677-1691.

26. Mangas-Sanjuan, V., Olah, J., et al. (2015) Tubulin acetylation promoting potency and absorption efficacy of deacetylase inhibitors. *Br J Pharmacol* **172,** 829-840.

27. Chopra, V., Quinti, L., et al. (2012) The sirtuin 2 inhibitor AK-7 is neuroprotective in Huntington's disease mouse models. *Cell Rep* **2,** 1492-1497.

28. Wu, F. L., Liu, W. Y., et al. (2016) Targeting endoplasmic reticulum stress in liver disease. *Expert review of gastroenterology & hepatology* **10,** 1041-1052.

29. Malhi, H. and Kaufman, R. J. (2011) Endoplasmic reticulum stress in liver disease. *Journal of hepatology* **54,** 795-809.

30. Hay, N. and Sonenberg, N. (2004) Upstream and downstream of mTOR. *Genes Dev* **18,** 1926-1945.

31. Ni, H. M., Bockus, A., et al. (2012) Activation of autophagy protects against acetaminophen-induced hepatotoxicity. *Hepatology* **55,** 222-232.

32. Borude, P., Bhushan, B., et al. (2018) Pleiotropic Role of p53 in Injury and Liver Regeneration after Acetaminophen Overdose. *Am J Pathol*.

33. Chen, W., Zhang, X., et al. (2017) Tethering Interleukin-22 to Apolipoprotein A-I

Ameliorates Mice from Acetaminophen-induced Liver Injury. *Theranostics* **7,** 4135-4148.

34. Wang, J., Koh, H. W., et al. (2017) Sirtuin 2 aggravates postischemic liver injury by deacetylating mitogen-activated protein kinase phosphatase-1. *Hepatology* **65,** 225-236.

35. Arteaga, M., Shang, N., et al. (2016) Inhibition of SIRT2 suppresses hepatic fibrosis. *Am J Physiol Gastrointest Liver Physiol* **310,** G1155-1168.

36. Lu, Z., Bourdi, M., et al. (2011) SIRT3-dependent deacetylation exacerbates acetaminophen hepatotoxicity. *EMBO Rep* **12,** 840-846.

37. Inoue, T., Nakayama, Y., et al. (2014) SIRT2 knockdown increases basal autophagy and prevents postslippage death by abnormally prolonging the mitotic arrest that is induced by microtubule inhibitors. *FEBS J* **281,** 2623-2637.

38. Park, S. H., Zhu, Y., et al. (2012) SIRT2 is a tumor suppressor that connects aging, acetylome, cell cycle signaling, and carcinogenesis. *Transl Cancer Res* **1,** 15-21.

39. Kim, H. S., Vassilopoulos, A., et al. (2011) SIRT2 maintains genome integrity and suppresses tumorigenesis through regulating APC/C activity. *Cancer Cell* **20,** 487-499.

40. Nie, H., Chen, H., et al. (2011) Silencing of SIRT2 induces cell death and a decrease in the intracellular ATP level of PC12 cells. *Int J Physiol Pathophysiol Pharmacol* **3,** 65-70.

41. Hoffmann, G., Breitenbucher, F., Schuler, M. and Ehrenhofer-Murray, A. E. (2014) A novel sirtuin 2 (SIRT2) inhibitor with p53-dependent pro-apoptotic activity in non-small cell lung cancer. *J Biol Chem* **289,** 5208-5216.

Figure legends

Fig. 1. APAP decreases Sirt2 levels in the mouse liver and ablation of Sirt2 ameliorates APAP-induced liver injuries in mice

(A) The livers of mice intraperitoneally injected with vehicle or APAP (500 mg/kg) for the indicated times were isolated, and liver homogenates were subjected to immunoblotting for Sirt2 and β-actin (loading control). (B) qRT-PCR analysis for the determination of Sirt2 mRNA levels. (C-D) Densitometric analysis of immunoblots, similar to those in (A). Ten-week-old WT and Sirt2 KO mice were injected with APAP (500 mg/kg). (E) Representative images, H&E analysis (magnification, 100×). The small panel images are enlarged photographs from the boxed areas (magnification, 200×), Quantitation of necrotic areas on H&E-stained mouse liver sections. (F) TUNEL analysis of liver sections and quantitation of TUNEL analysis. (G) Serum levels of alanine transaminase (=GPT). (H) Serum levels of GOP. Investigation of the increased hepatotoxicity in mice treated with vehicle, APAP, or AGK2 (Sirt2 inhibitor). Ten-week-old WT and Sirt2 KO mice were injected with AGK2 (1 mg/kg) 2 h prior to APAP (500 mg/kg) administration, and plasma and livers were collected 12 h after APAP injection. (I) Representative images from H&E analysis and Quantitation of the necrotic area. (J) TUNEL analysis and Quantitation. (K) Serum levels of alanine transaminase (=GPT). (L) Serum levels of GOP. Data represent the mean ± SD from three independent experiments. *$p < 0.05$, **$p < 0.01$, N.S, not significant.

Fig. 2. The inactivation of Sirt2 attenuates ER stress in APAP-induced liver injuries in

mice

(A-D) The livers of mice intraperitoneally injected with vehicle or APAP (500 mg/kg) for the indicated times were isolated, and qRT-PCR analysis for the determination of Grp78, PERK, ATF4, and IRE1α mRNA levels. (E-H) Sirt2 WT or Sirt2 KO mice 12 h after an intraperitoneal injected with vehicle or APAP (500 mg/kg). qRT-PCR analysis for the determination of Grp78, PERK, ATF4, and IRE1α mRNA levels. (I-L) The livers of mice intraperitoneally injected with vehicle, APAP (500 mg/kg, i.p), and AGK2 (1 mg/kg) for 12 h were isolated, and qRT-PCR analysis for the determination of Grp78, PERK, ATF4, and IRE1α mRNA levels. Data represent the mean ± SD from three independent experiments. *p < 0.05.

Fig. 3. The APAP-induced S6K1 phosphorylation is inhibited in the livers of Sirt2-inactivated mice

(A) The livers of mice intraperitoneally injected with vehicle or APAP (500 mg/kg) for the indicated times were isolated, and immunoblot analysis for p-S6K1, S6K1, p-S6, and S6. (B-C) Densitometric analysis. (D-F) Sirt2 WT or Sirt2 KO mice 12 h after an intraperitoneal injected with vehicle or APAP (500 mg/kg), immunoblot analysis for Sirt2, p-S6K1, S6K1, p-S6, and S6. Densitometric analysis (D). (G) The livers of mice intraperitoneally injected with vehicle, APAP (500 mg/kg), AGK2 (1 mg/kg) for 12 h were isolated, and immunoblot analyses for p-S6K1, S6K1, p-S6, and S6. (H-I) Densitometric analysis. Data represent the mean ± SD from three independent experiments. *p < 0.05.

Fig. 4. Sirt2 regulates the phosphorylation of S6K1 through S6K1 deacetylation in APAP-treated mouse livers

Immunoblots of immunoprecipitates and whole-cell lysates from lysates of (A) HEK293 cells transfected with S6K1 and Flag-Sirt2 (F-SIRT2) vectors subjected to immunoprecipitation with an anti-S6K1 antibody. (B) HEK293 cells transfected with an S6K1, F-SIRT2, and a Sirt2 (H187Y) catalytic dead mutant vector subjected to immunoprecipitation with antibodies against acetyllysine, S6K1, or Flag. (C) HEK293 cells transfected with an HA-S6K1 (H-S6K1) or a Flag-Sirt2 vector subjected to immunoprecipitation with antibodies against Flag. (D) HEK293 cells transfected with H-S6K1, F-SIRT2, and F-SIRT2 (H187Y) vectors subjected to immunoprecipitation with antibodies against acetyllysine, or HA. (E) Sirt2 WT or Sirt2 KO mouse livers, following treatment with APAP for 12 h, subjected to immunoprecipitation with an anti-S6K1 antibody. (F) Sirt2 WT mouse livers, following treatment with APAP or AGK2 for 12 h, subjected to immunoprecipitation with an anti-S6K1 antibody.

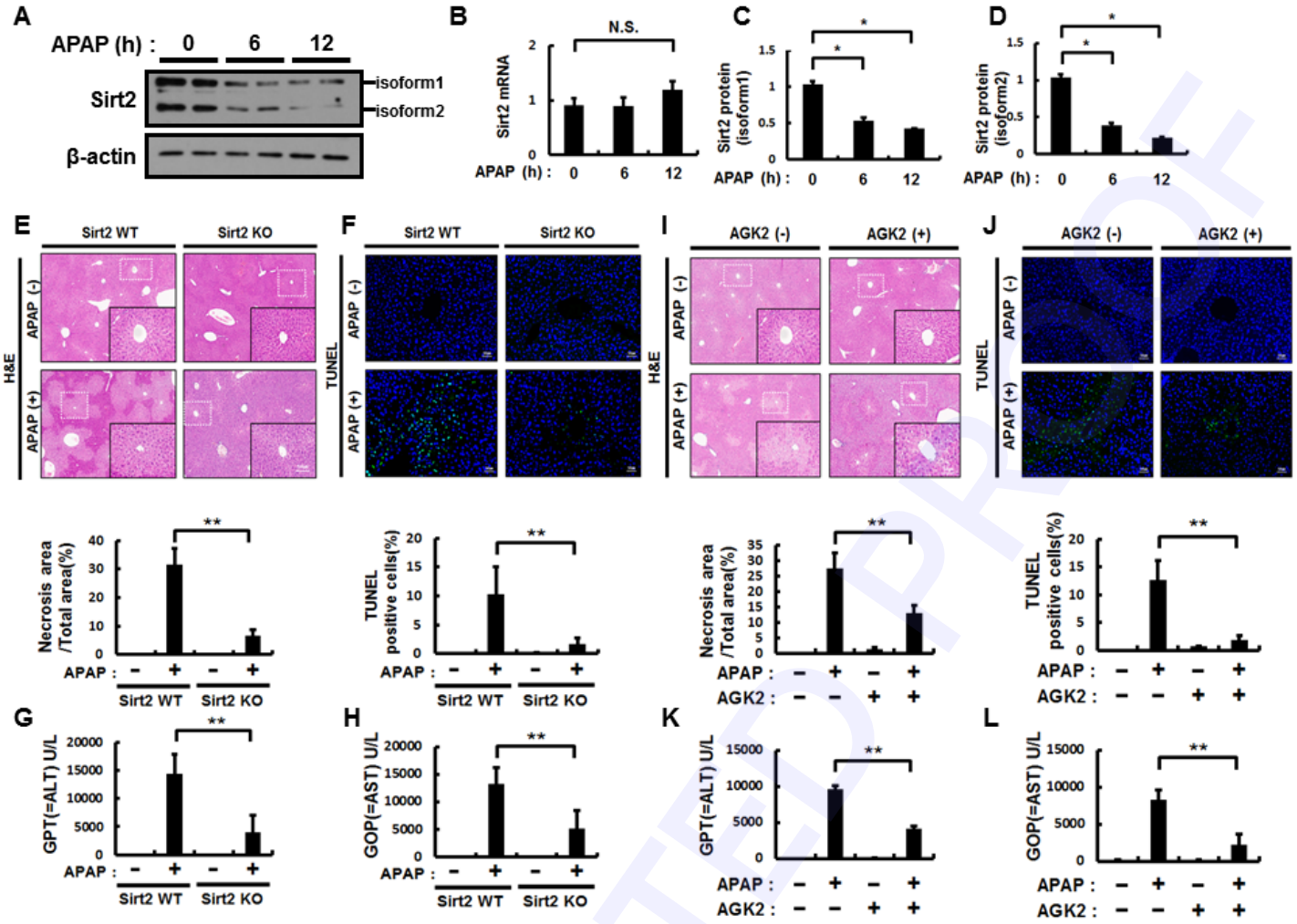

Lee, Fig.1

Fig. 1.

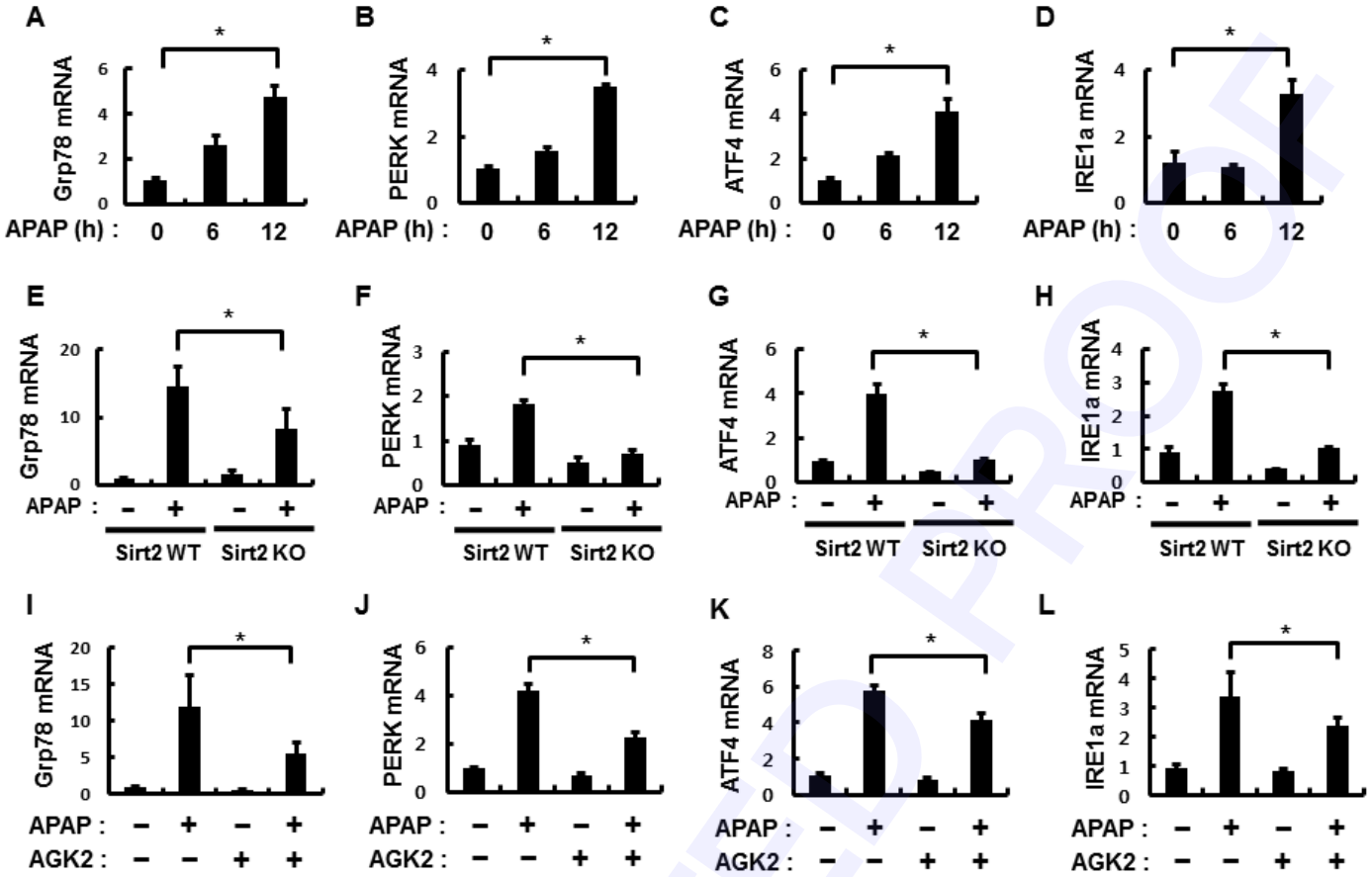

Lee, Fig.2

Fig. 2.

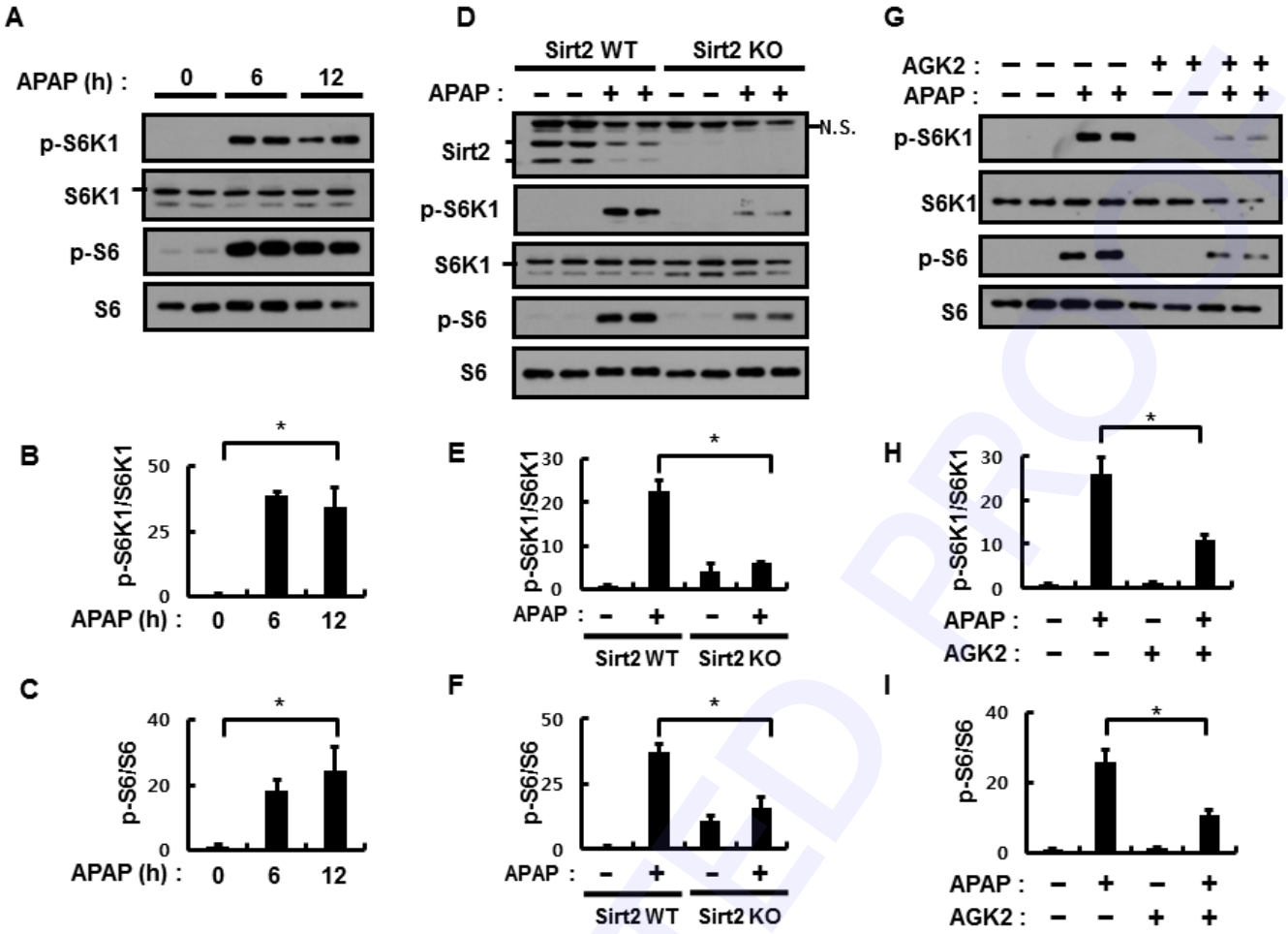

Lee, Fig.3

Fig. 3.

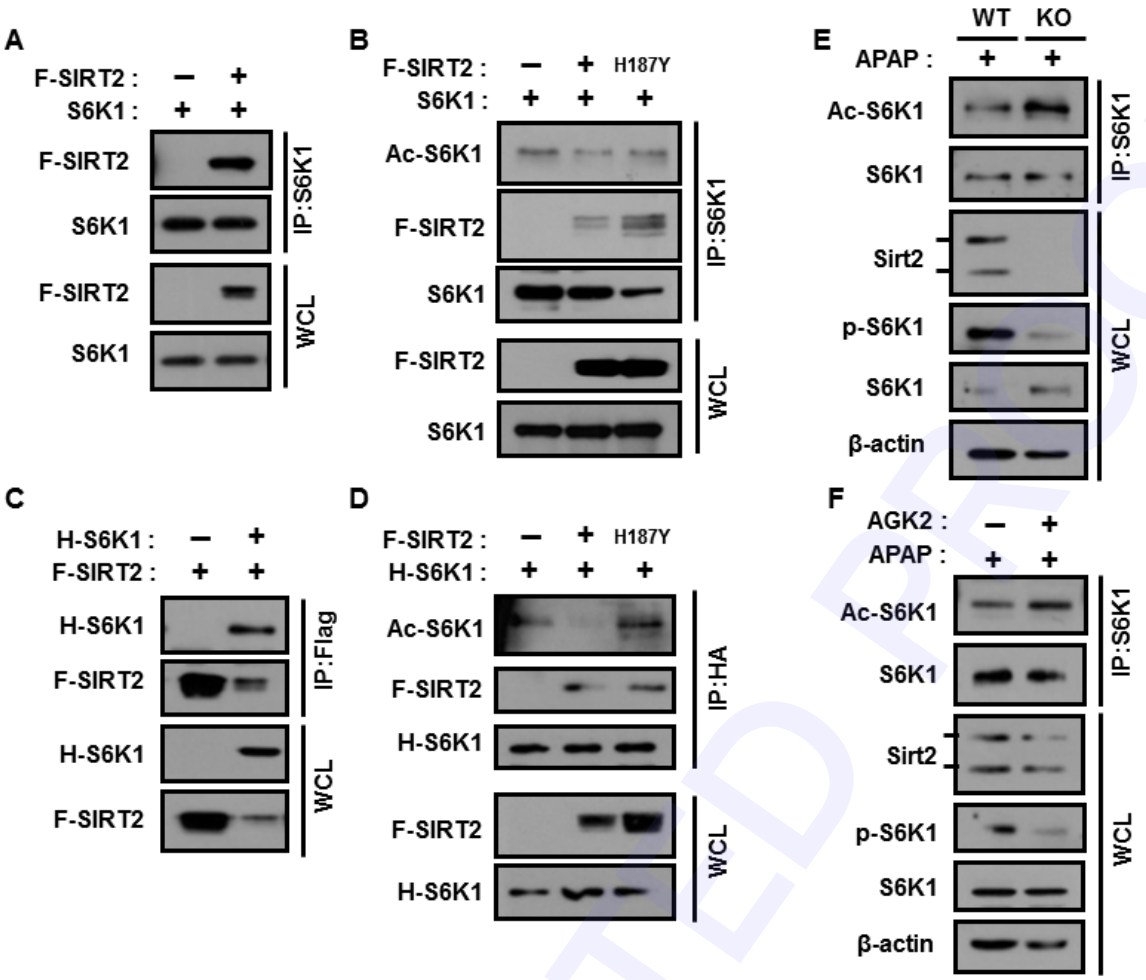

Lee, Fig.4

Fig. 4.

Inactivation of Sirtuin2 protects mice from acetaminophen-induced liver injury: possible involvement of ER stress and S6K1 activation

Da Hyun Lee[1,2#], Buhyun Lee[1,2#], Jeong Su Park[2], Yu Seol Lee[1,2], Jin Hee Kim[6], Yejin Cho[2], Yoonjung Jo[3], Hyun-Seok Kim[3], Yong-ho Lee[4,5]*, Ki Taek Nam[1,2]*, and Soo Han Bae[2]*

[1]Brain Korea 21 PLUS Project for Medical Science, Yonsei University;

[2]Severance Biomedical Science Institute, Yonsei Biomedical Research Institute, Yonsei University College of Medicine, 50 Yonsei-ro, Seodaemun-gu, Seoul 03722, Republic of Korea;

[3]Department of Bioinspired Science, Ewha Womans University, Seoul 120-750, Korea;

[4]Division of Endocrinology and Metabolism, Department of Internal Medicine, Yonsei University College of Medicine, 50-1, Yonsei-ro, Seodaemun-gu, Seoul 03722, Republic of Korea;

[5]Institute of Endocrine Research, Yonsei University College of Medicine, 50-1, Yonsei-ro, Seodaemun-gu, Seoul 03722, Republic of Korea;

[6]Brain Korea 21 PLUS Project for Medical Science, Yonsei University College of Medicine, 50-1 Yonsei-ro, Seodaemun-gu, Seoul, 03722, Republic of Korea

[#]These authors contributed equally to this work.

Corresponding authors:

Soo Han Bae, Ph.D

Severance Biomedical Science Institute, Yonsei Biomedical Research Institute, Yonsei University College of Medicine, 50-1 Yonsei-ro, Seodaemun-gu, Seoul 03722, Republic of

Korea. Tel.: +82-2 2228-0756; Fax: +82-2-2227-8129; E–mail address: soohanbae@yuhs.ac

Ki Taek Nam, DVM, Ph.D

Severance Biomedical Science Institute, Yonsei Biomedical Research Institute, Yonsei University College of Medicine, 50-1 Yonsei-ro, Seodaemun-gu, Seoul 03722, Republic of Korea. Tel.: +82-2 2228-0754; Fax: +82-2-2227-8129; E–mail address: KITAEK@yuhs.ac

Yong-ho Lee, M.D., Ph.D.

Division of Endocrinology and Metabolism, Department of Internal Medicine, Yonsei University College of Medicine, 50-1, Yonsei–ro, Seodaemun–gu, Seoul 03722, Republic of Korea. Tel.: +82-2-2228-1943; Fax: +82-2-393-6884; E–mail address: yholee@yuhs.ac

Supplementary Experimental Procedures

Animals

Ten-week-old C57BL/6J male mice were purchased from Orient Bio (Sungnam, Korea) and Sirt2 knockout (Sirt2 KO) mice were generated as previously described (48). Sirt2 KO mice of C57BL/6 background were kindly provided by Dr. H. S. Kim (Ewha Womans University, Seoul, Korea) (48). The mice had free access to food and water and were maintained at a temperature of 23 ± 2 °C, a humidity of 60 ± 10%, and a 12-hour light/dark cycle. Prior to APAP and AGK2 administration, mice were fasted for 15 h but had free access to water. APAP was dissolved in warm distilled water (60 °C) and intraperitoneally injected (500 mg/kg) into overnight-fasted mice to induce hepatitis. AGK2 was dissolved in dimethyl sulfoxide (DMSO) and intraperitoneally injected (1 mg/kg) 2 h prior to APAP administration. At 6 and 12 h after injection, the mice were anesthetized and killed; blood was collected via cardiac puncture. Tissues were harvested and either snap frozen in liquid nitrogen and stored at −70 ºC or fixed in formalin and embedded in paraffin. All animal studies were approved by

the Animal Care and Use Committee of the Yonsei University College of Medicine.

Immunohistochemistry

For immunohistochemistry, sample were fixed with 4% paraformaldehyde and embedded in paraffin. Next, 10-μm sections were deparaffinized and sequentially rehydrated. Antigen retrieval was performed using the Target Retrieval solution, pH 6 (S1699, DAKO, Glostrup, Denmark) in a pressure cooker for 15 min. After cooling on ice for at least 1 h, the sections were incubated in 3% H_2O_2 for 30 min to block endogenous peroxidase activity. The sections were washed two times with PBS and incubated with Protein block serum-free (DAKO, X0909) for 2 h at room temperature for reducing nonspecific signals. Following incubation with primary antibodies, overnight at 4 °C in the presence of 3-nitrotyrosine (Millipore, Daejeon, Korea), and 3 washes in PBS, the sections were incubated with horseradish peroxidase-conjugated rabbit secondary antibodies (DAKO, K4003) for 15 min at room temperature. For immunohistochemistry, **3,3'**-diaminobenzidine (DAKO, K3468) was used for development and Mayer's Haematoxylin (DAKO, S3309) was used for counterstaining.

Statistical analysis

Data in the graphs were analysed using a two-tailed Student's t test for comparisons between 2 groups, or a one-way ANOVA with Tukey's honest significant difference post hoc test for multiple comparisons (SPSS 12.0K for Windows, SPSS, Chicago, IL) to determine statistical significance. A value of $P < 0.05$ was considered significant.

Biochemical analyses

Serum levels of alanine aminotransferase (GPT) and aspartate aminotransferase (GOT) were measured by ELISA (BioAssay Systems, Hayward, CA, USA).

Histological analysis

Liver tissue fixed with 4% buffered formalin solution was embedded in paraffin and sectioned. Sections (10 μm thick) were then depleted of paraffin, subjected to H&E staining, and examined in a blinded manner for grading the ballooning degeneration of hepatocytes. 0 = none, 1 = few balloon cells, 2 = many cells/prominent ballooning (48). The liver necrotic area was diagnosed by a pathologist (K.T.N) and quantified with an Aperio Imagescope (Leica Biosystems, Richmond) and the necrotic area (%) was calculated using the necrosis area/total area of the liver section.

Immunoblotting

Cells were homogenized in a lysis buffer containing 20 mM HEPES-KOH (pH 7.9), 125 mM NaCl, 10% glycerol, 0.3% Triton™ X-100, 1 mM EDTA, 0.5% NP-40, 10 mM β-phosphoglycerate, 1 mM Na_3VO_4, 5 mM NaF, 1 mM aprotinin, 1 mM leupeptin, and 1 mM phenylmethanesulfonylfluoride. Following centrifugation, the resulting supernatants were subjected to sodium dodecyl sulphate polyacrylamide gel electrophoresis after protein quantification. Samples were heated at 95 °C for 5 min and separated electrophoretically on a 12% or 14% SDS-polyacrylamide gel. Subsequently, the separated proteins were transferred to polyvinylidene fluoride membranes and incubated overnight with the indicated primary antibodies at 4 °C. After incubation with horseradish peroxidase-conjugated secondary antibodies, proteins were detected with enhanced chemiluminescence lighting solution (Young in Frontier Co. Ltd, Seoul, Korea).

Immunoprecipitation (IP) analysis

For immunoprecipitation, HEK293 cells were lysed in a lysis buffer containing 50 mM Tris-

HCl (pH 7.5), 150 mM NaCl, aprotinin, leupeptin and 1% Nonidet P-40. The cell lysates were centrifuged, and the resulting supernatants were subjected to immunoprecipitation with antibodies against FLAG or HA, using protein G-Sepharose beads, as previously described (Woo et al., 2009). For immunoblot analysis, cell lysates or immunoprecipitates were subjected to SDS-PAGE gel electrophoresis; the separated proteins were transferred to a polyvinylidene fluoride membrane, which was incubated first with primary antibodies and then with horseradish peroxidase-conjugated secondary antibodies, and enhanced chemiluminescence reagents (Young in Frontier).

Electron microscopy

Samples were fixed for 12 h in 2% glutaraldehyde-paraformaldehyde in 0.1 M phosphate buffer (PBS, pH 7.4) and washed in 0.1 M PBS. They were post-fixed with 1% OsO4 dissolved in 0.1 M PBS for 2 h, dehydrated in an ascending gradual series of ethanol and infiltrated with propylene oxide. Specimens were embedded using the Poly/Bed 812 kit (Polysciences, Warrington, PA). After embedding in pure fresh resin, the sections were polymerized at 65 °C in an electron microscopy oven (TD-700, DOSAKA, Kyoto, Japan) for 24 h. Sections of about 200~250 nm in thickness were initially cut and stained with toluidine blue (Sigma, St Louis, MO T3260) for light microscopy. Next, 70-nm thin sections were double stained with 6% uranyl acetate (EMS, Hatfield, PA, 22400) for 20 min and lead citrate (Fisher, Pittsburgh, PA) for 10 min for contrast staining. There sections were cut using a LEICA EM UC-7 (Leica Microsystems, Weltzar, Germany) with a diamond knife (Diatome) and transferred to copper and nickel grids. All thin sections were observed by transmission electron microscopy (JEM-1011, JEOL, Akishima, Japan) at the acceleration voltage of 80 kV using a Camera-Megaview III (Soft imaging system, Munster, Germany)

Terminal deoxynucleotidyl transferase-mediated dUTP nick-end labelling (TUNEL) analysis

Liver sections were subjected to TUNEL analysis using an *In Situ* Cell Death Detection Kit, TMR Red (Roche, Basel, Switzerland). Fluorescence signals were detected with a confocal microscope (LSM 700, Zeiss, Jena, Germany), and the frequency of apoptotic cells in the sections was quantified by determining the percentage of TUNEL-positive cells in 10 random microscopic fields per specimen.

Antibodies and reagents

The following antibodies were used: anti-Sirt2 (Sigma S8447); anti-p70S6K (Cell Signaling, Danvers, MS #9202); anti-phospho-p70S6K (Cell Signaling #9205); anti-S6 (Cell Signaling 2217S); anti-phospho-S6 (Cell Signaling 2211S); anti-acetylated lysine (Cell Signaling #9441); anti-Bip/Grp78 (BD Bioscience, Franklin Lakes, NJ, 610979); anti-nitrotyrosine (Millipore, Billerica, MS, 06-284); anti-mTOR (Cell Signaling #2972); anti-phospho-mTOR (Cell Signaling #2971); anti-β-actin (Abclonal, Cambridge, MA, AbC-2002-1); anti-Flag (Millipore MAB3118); anti-HA (Bethyl Laboratories, Montgomery, TX, A190-108A). APAP and dimethyl sulfoxide (DMSO), cycloheximide (CHX), chloroquine (CQ), and MG132 were purchased from Sigma Aldrich.

Expression Vectors

Flag-tagged human Sirt2 and the Sirt2 catalytic mutant (H187Y) cDNA were kindly provided by Dr. Ahn. HA-tagged S6K1 cDNA was purchased from Addgene (Cambridge, MA). S6K1 cDNA was purchased from the Korea Laboratory Accreditation Scheme (KOLAS).

Cell culture

HEK293 cells and normal liver cells (AML12 cells) were maintained under 5% CO_2 at 37 °C in Dulbecco's modified Eagle's medium supplemented with 10% foetal bovine serum, 1% penicillin, and 1% streptomycin.

Quantitative RT-PCR analysis

Total RNA was isolated from cultured cells using the TRIzol® reagent and reverse transcribed with a TAKARA cDNA synthesis kit (TAKARA, Shiga, Japan). The resulting cDNA was subjected to quantitative PCR analysis using SYBR® Green and an ABI PRISM 7700 system. Ribosomal RNA (18S) was used as an internal control (Bae et al., 2013). The sequences of the primers for mouse cDNAs (forward and reverse, respectively) were as follows: Grp78 primers, 5′-GAAAGGATGGTTAATGATGCTGAG-3′ and 5′-GTCTTCAATGTCCGCATCCTG-3′; PERK, 5′-TCTTGGTTGGGTCTGATGAAT-3′ and 5′-GATGTTCTTGTGTAGTGGGGG-3′; ATF4, 5′-ACACAGCCCTTCCACCTC-3′ and 5′-CACGGGAACCACCTGGAG-3′; IRE1α, 5′-CTGTGGTCAAGATGGACTGG-3′ and 5′-GAAGCGGGAAGTGAAGTAGC-3′; 18S, 5′-CGCTCCCAAGATCCAACTAC-3′ and 5′-CTGAGAAACGGCTACCACATC-3′. Real-time PCR conditions were as follows: pre-denaturation at 95 °C for 10 min, followed by 40 cycles of denaturation at 95 °C for 15 s, and annealing/extension at 60 °C for 1 min.

Supplementary Figure Legends

Supplementary Fig.1. APAP decreases the protein levels of Sirt2

(A) Normal liver cells (AML12 cells) treated with APAP (10 mM) and incubated with or without CHX (5 μg/ml) were lysed and subjected to immumoblot analysis with antibodies against Sirt2 and β-actin (loading control). (B-C) Densitometric analysis of Sirt2 isoform1 and 2 immunoblots obtained. (D) AML12 cells treated with APAP and incubated with or

without CQ were lysed and subjected to immunoblot analysis with antibodies against Sirt2 and β-actin (loading control). (E-F) Densitometric analysis of Sirt2 isoform1 and 2 immunoblots obtained. (G) AML12 cells treated with APAP and incubated with or without MG132 were lysed and subjected to immunoblot analysis with antibodies against Sirt2 and β-actin (loading control. (H-I) Densitometric analysis of Sirt2 isoform1 and 2 immunoblots obtained. Data are presented as means ± SD from three independent experiments. **$p<0.01$, *$p<0.05$, and N.S, not significant.

Supplementary Fig.2. The ablation of Sirt2 ameliorates the APAP-induced liver injury in the mouse liver

Increased liver injury in mouse liver with treatment of APAP for 6h is determined. (A) Representative images from H&E and Masson's trichrome staining (magnification, ×100). (B) Quantitation of Necrosis area in H&E staining of mouse liver sections. (C) TUNEL analysis of liver sections (D) Quantitation of TUNEL analysis. (E) Serum levels of ALT (=GPT). (F) Serum levels of AST (=GOP). Data are mean ± SD from three independent experiments. *$p<0.05$.

Supplementary Fig.3. The ablation of Sirt2 alleviates APAP-induced liver injury and mitochondrial damage in mouse liver

Increased liver injury in mouse liver with treatment of APAP for 12h is determined. (A) 3-nitrotyrosine (3-NT) measured by immunohistochemical (IHC) stating. (B) Quantitation of IHC analysis. (C) Mitochondrial detection using electron microscopy (EM). Data are presented as means ± SD from three independent experiments. **$p<0.01$.

Supplementary Fig.4. The ablation of Sirt2 attenuates APAP-induced liver in mouse

liver

Increased liver injury in mouse liver with treatment of APAP for 6h is determined. (A) 3-nitrotyrosine (3-NT) measured by immunohistochemical (IHC) stating. (B) Quantitation of IHC analysis. Data are presented as means ± SD from three independent experiments. *p<0.05.

Supplementary Fig.5. The pharmacological inactivation of Sirt2 alleviates APAP-induced liver injury in mouse liver

Increased hepatotoxicity in mice with treatment of vehicle, APAP, or AGK2 (Sirt2 inhibitor) was investigated. (A) 3-nitrotyrosine (3-NT) measured by immunohistochemical (IHC) stating. (B) Quantitation of IHC analysis. (C) Mitochondrial detection using electron microscopy (EM). Data are presented as means ± SD from three independent experiments. **p<0.01.

Supplementary Fig.6. Ablation of Sirt2 attenuates ER stress in the APAP-induced liver injury in mouse.

(A) Immunoblot analysis of Sirt2, p-S6K1, S6K1, and β-actin (loading control) in mice with treatment of vehicle or APAP. (B) Densitometric analysis of p-S6K1/ S6K1 immunoblots was obtained. Total mRNA isolated liver from mice treated as described in (A) was subjected to qRT-PCR analysis for mRNAs of BiP/Grp78 (C) and ATF4 (D). Data are mean ± SD from three independent experiments. *P<0.05.

Supplementary Fig.7. Sirt2 has no effect in phosphorylation of mTOR

(A) Immunoblot analysis of p-mTOR and mTOR in mice with treatment of vehicle or APAP.

(B) Densitometric analysis of p-mTOR/mTOR immunoblots was obtained. (C) Immunoblot analysis of p-mTOR and mTOR in mice with treatment of vehicle, APAP, or AGK2 (Sirt2 inhibitor) (D) Densitometric analysis of of p-mTOR/mTOR immunoblots was obtained. Data are mean ± SD from three independent experiments. N.S, not significant.

Supplementary Fig.8. Model for the role of Sirt2 inactivation in APAP-induced liver injury in mouse

See text for details.

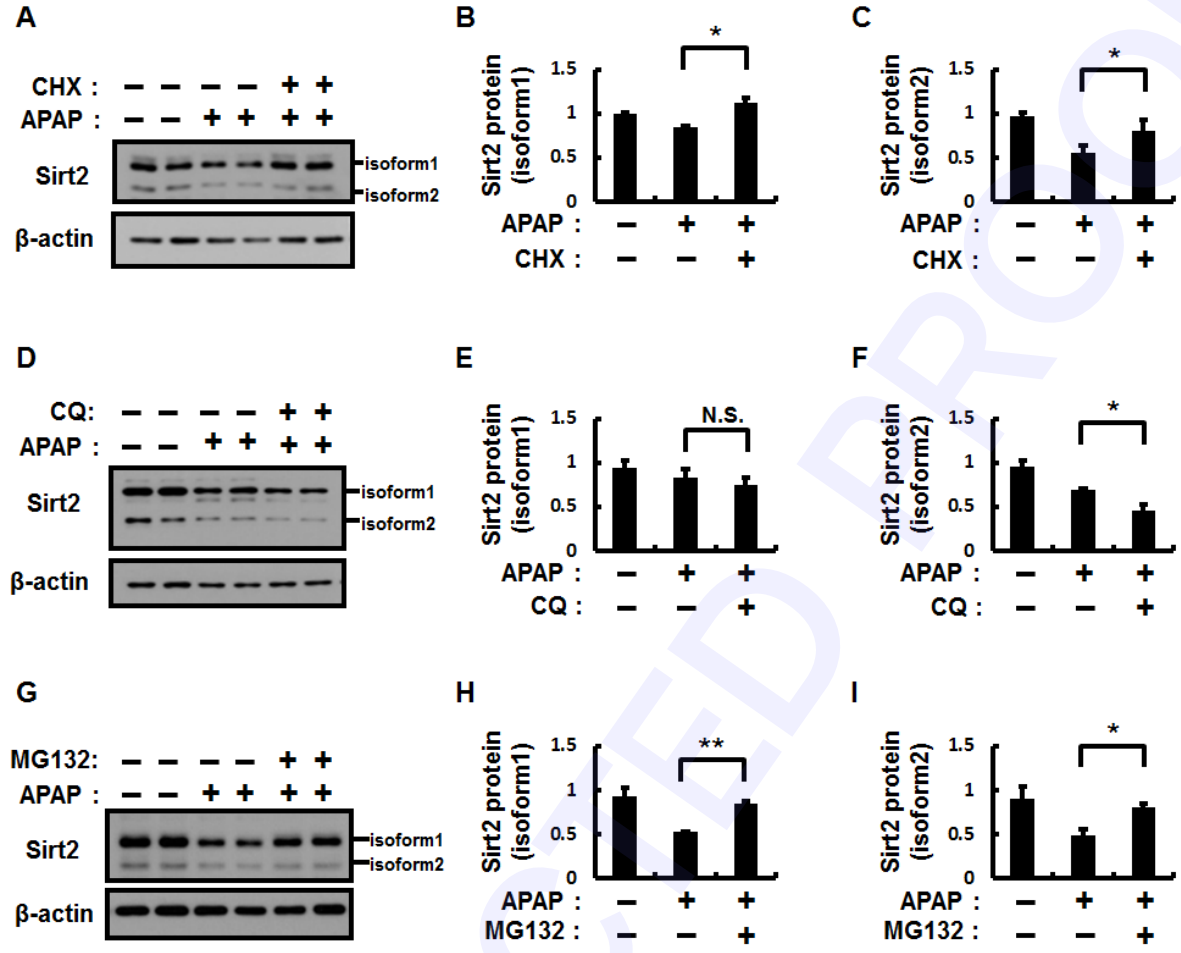

Supplementary Fig.1.

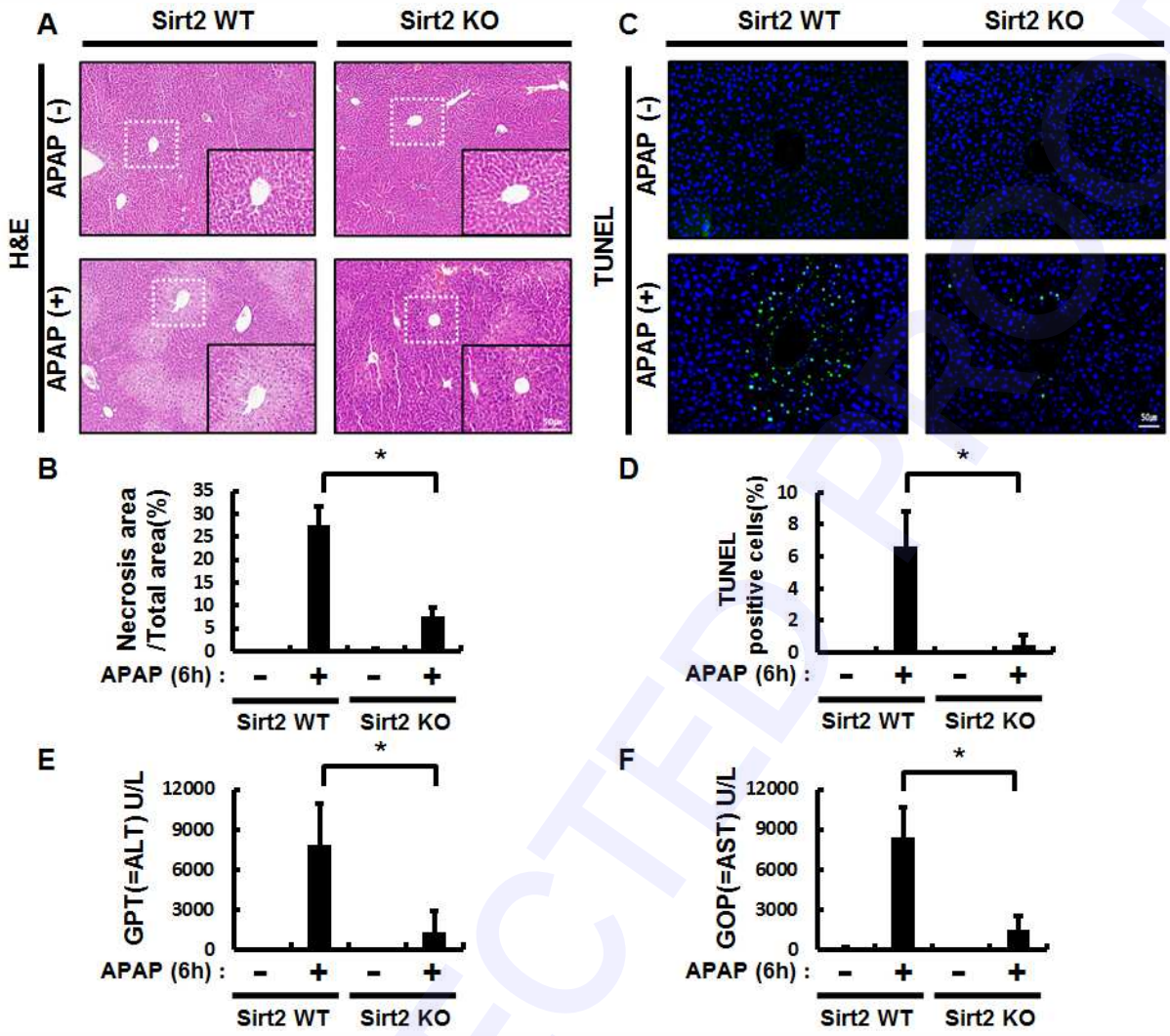

Supplementary Fig.2.

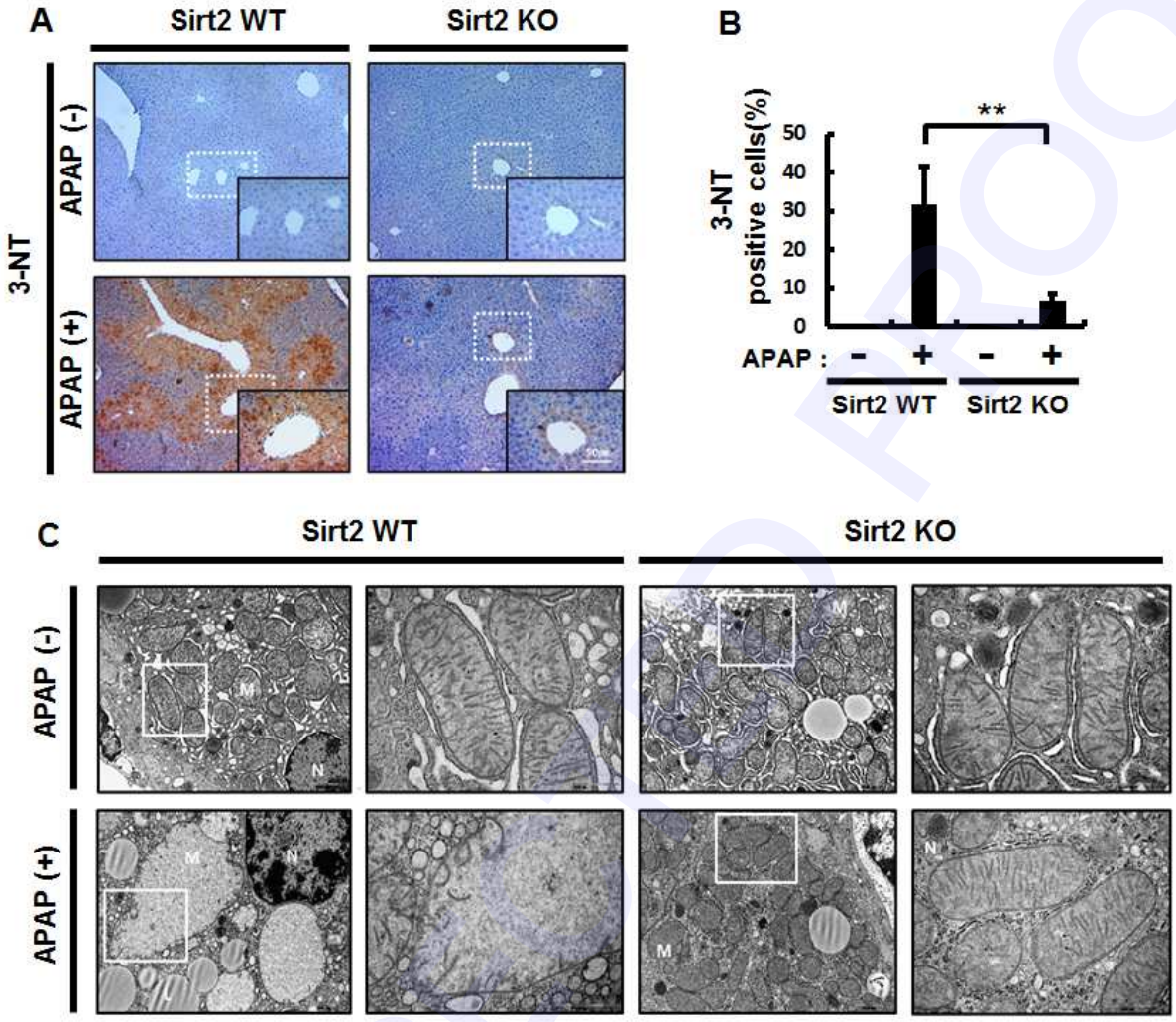

Supplementary Fig.3.

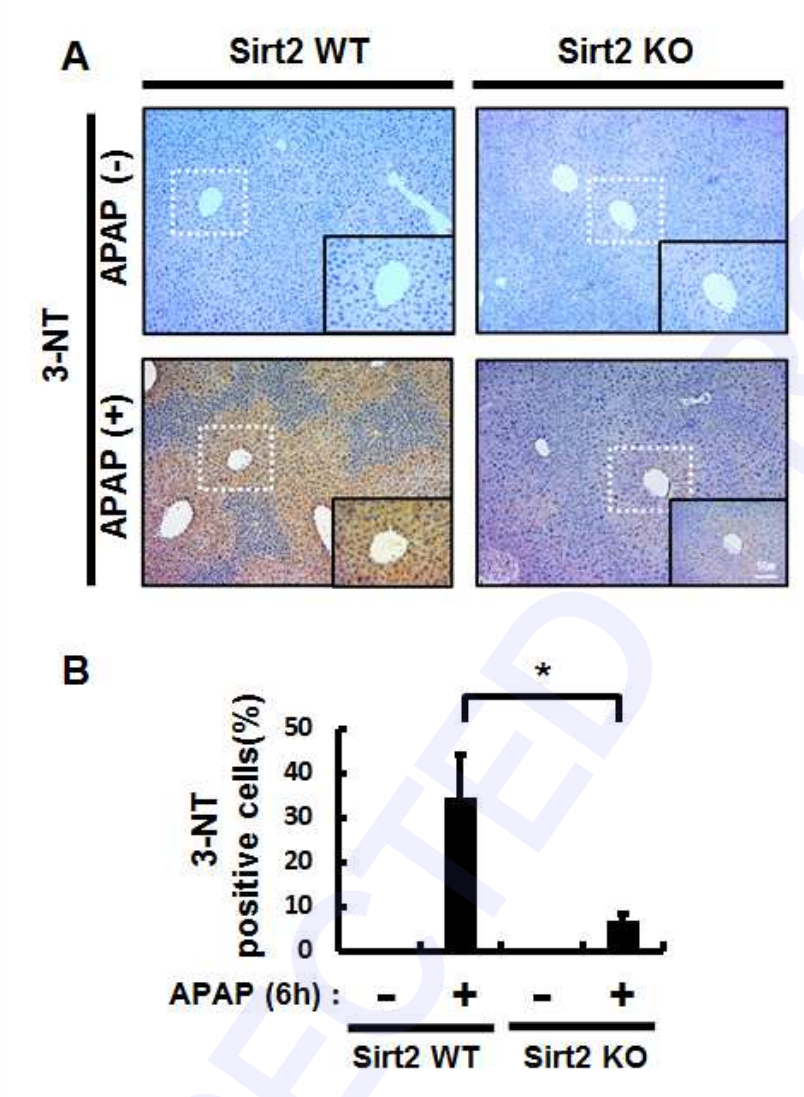

Supplementary Fig.4.

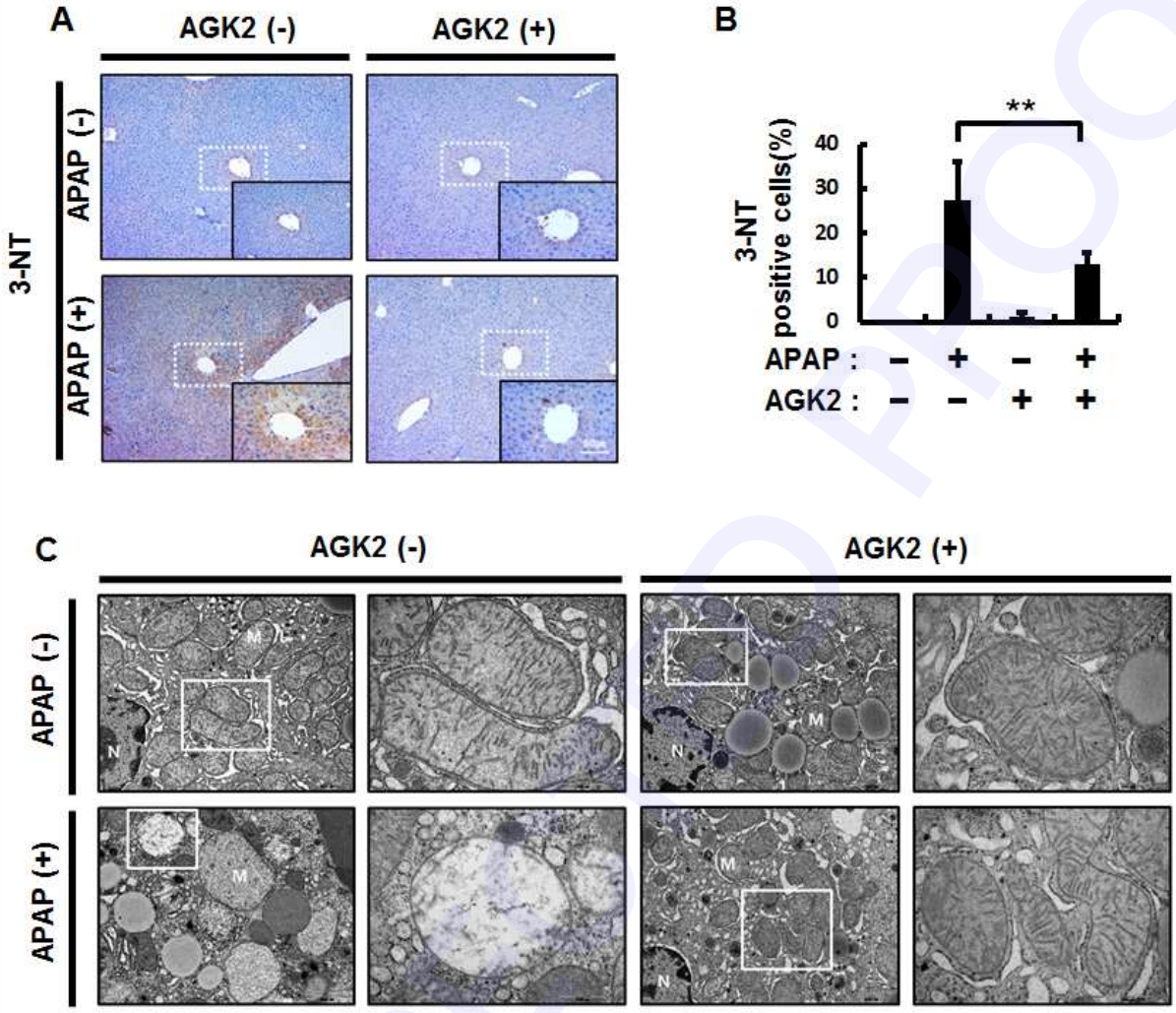

Supplementary Fig.5.

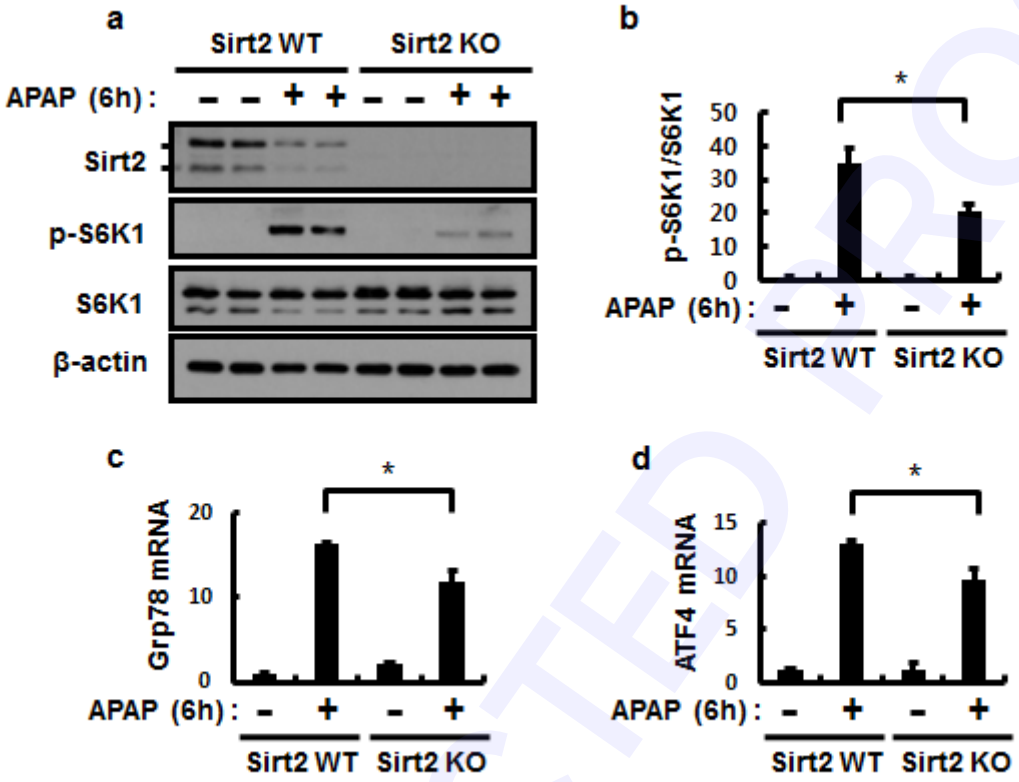

Supplementary Fig.6.

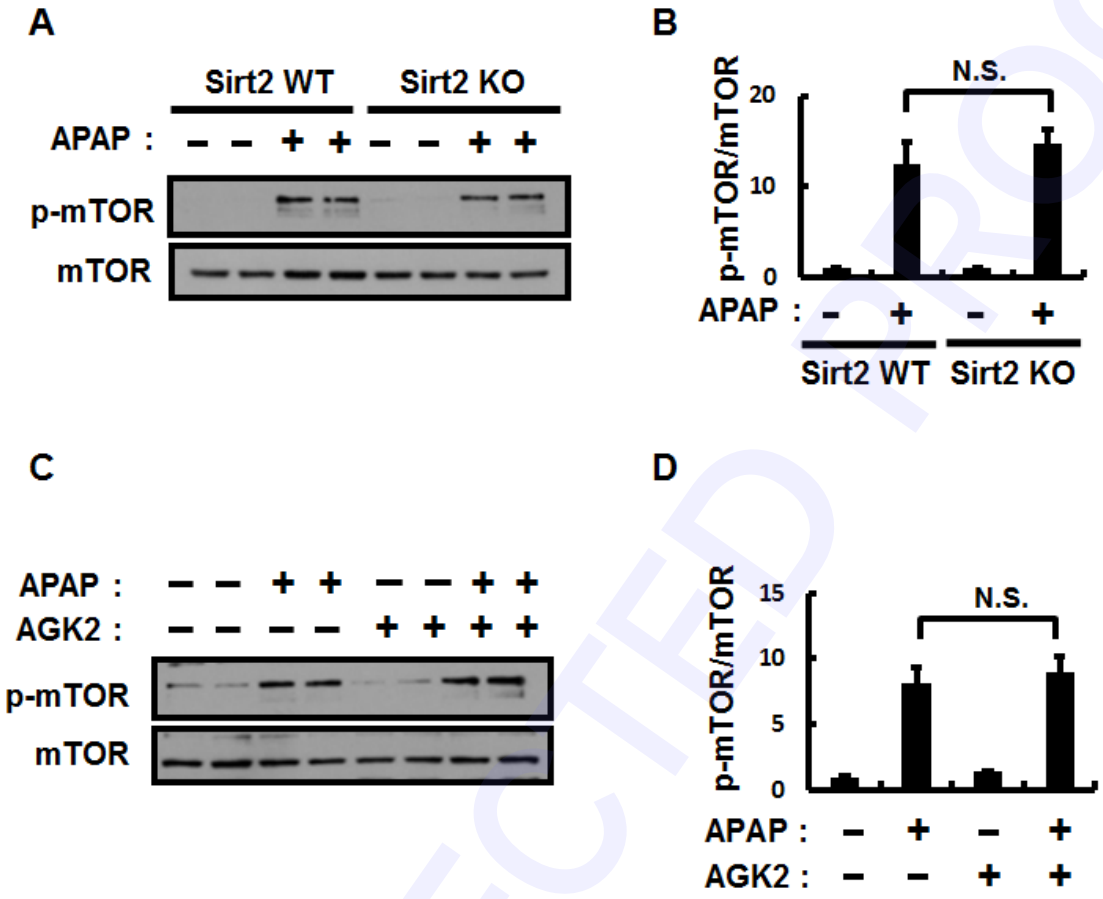

Supplementary Fig.7.

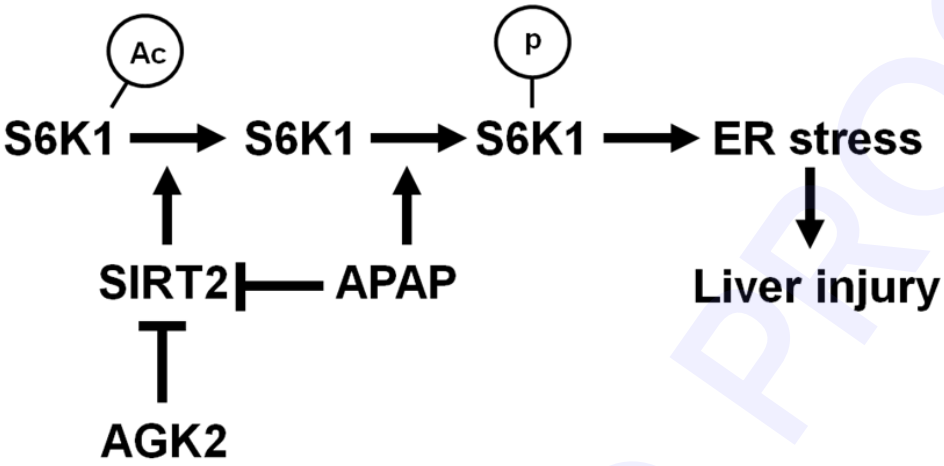

Supplementary Fig.8.